Journal of Power Sources 216 (2012) 409–416

Contents lists available at SciVerse ScienceDirect

Journal of Power Sources

journal homepage: www.elsevier.com/locate/jpowsour

# Stability of solid oxide fuel cell anodes based on YST–SDC composite with Ni catalyst

Pramote Puengjinda, Hiroki Muroyama, Toshiaki Matsui, Koichi Eguchi*

*Department of Energy and Hydrocarbon Chemistry, Graduate School of Engineering, Kyoto University, Nishikyo-ku, Kyoto 615-8510, Japan*

## HIGHLIGHTS

- The use of Ni/YST–SDC ceramic anode was proposed to replace Ni-based cermet.
- Addition of nickel enhances the electrochemical performance without drawback effects.
- The excellence of YST–SDC ceramic framework could maintain the stable performance.
- Ni/YST–SDC offers certain advantages and highly stable performance in severe conditions.

## ARTICLE INFO

*Article history:*
Received 14 February 2012
Received in revised form
15 May 2012
Accepted 28 May 2012
Available online 1 June 2012

*Keywords:*
Ceramic anodes
Solid oxide fuel cells
Stable performance
Severe conditions
Redox tolerance

## ABSTRACT

Ceramic material based on composite of yttria-doped $SrTiO_3$ (YST) and samaria-doped ceria (SDC) incorporated with Ni catalyst has been evaluated as an anode of solid oxide fuel cell to substitute the use of conventional Ni-based cermets. The results indicated the advantages of suitable Ni addition which could remarkably enhance the electrochemical performance of anode due to the superior in catalytic activity of SDC and Ni towards fuel oxidation. Temperature-programmed reduction (TPR) profiles indicated the existence of bulk-free and interacted NiO in the composites. The cells with Ni/YST–SDC (20 wt% NiO) anodes exhibited stable performance in the prolong operation with tremendously severe conditions in methane fuel with low steam to carbon ratio (S/C = 0.1) and highly humidified hydrogen fuel (40% $H_2O$–$H_2$) compared with the conventional Ni-based cermets. Small amount of deposited carbon was observed and played insignificant effects on the electrochemical performance after the operation for 100 h. The stable performance was ascribable to the excellence in YST–SDC ceramic framework that effectively suppressed the carbon formation. Furthermore, the Ni/YST–SDC anode showed high tolerance in encountering with the redox cycles. From these results, Ni/YST–SDC composite is considered to be a promising candidate for SOFC anode material operating in severe conditions.



## 1. Introduction

Regarding to the renewed interest in alternative energy sources, solid oxide fuel cells (SOFCs), which are typically operated at high temperatures, have attracted a great attention among other types of fuel cells due to the relatively high efficiency. These aspects serve the use of SOFC to an alternative and more commercially attractive application in a wide range of cleaner energy. The merit of high operating temperature (800–1000 °C) thermodynamically offers fuel flexibility in particular hydrocarbon internal reforming directly without the requirement of external reforming system or the use of noble metal catalysts to promote the reactions [1]. In contrast, high-operating temperatures critically limit the types of compatible materials composed in the cell and the development of potential materials is still required to meet the satisfied characteristics. The composite between nickel and yttria-stabilized zirconia (Ni–YSZ) or Ni-based cermet which typically contains a high volume fraction of Ni is the most prevalent because it possesses high electronic conductivity coexisting with the catalytic activity. However, a high fraction of Ni induces some catastrophic problems in the system such as the electrode sintering and coking formation when hydrocarbons are treated at high temperature [2]. To overcome these problems, therefore, it is necessary to develop alternative anode materials, which provide not only the compatibility with the SOFC components but also the feasibility of the direct fuel conversion with stability in long-term operation.

* Corresponding author. Tel.: +81 75 383 2519; fax: +81 75 383 2520.
*E-mail address:* eguchi@scl.kyoto-u.ac.jp (K. Eguchi).

0378-7753/$ – see front matter © 2012 Elsevier B.V. All rights reserved.
http://dx.doi.org/10.1016/j.jpowsour.2012.05.089

Doped $SrTiO_3$ ceramics including lanthania- or yttria-doped $SrTiO_3$ ($La_xSr_{1-x}TiO_3$ (LST) or $Y_xSr_{1-x}TiO_3$ (YST)) have been studied as a potential candidate for anode material because of their high electronic conductivity under reducing conditions [3–10]. Recently, the ceramic composite of YST–SDC has been developed as an alternative anode material, which showed the excellence in both electrocatalytic activity and mechanical compatibility with YSZ electrolyte [11]. Although the ceramic composite of YST–SDC has the potential to offer properties as an alternative anode, its electrochemical performance is lower than that of the conventional Ni-based cermets. For this case, a small amount of metallic catalyst (e.g. Ni, Pt) can be introduced into the composite to improve the electrochemical performance to an acceptable level without the drawback effects. In practical applications, the primary difficulty in operation with hydrocarbon fuels is a deactivation of anode due to the carbon deposition. The carbon deposition occurs rapidly with the use of hydrocarbon fuels leading to the performance deterioration. The criteria of carbon deposition at the operating conditions can be determined by thermodynamic equilibrium compositions presented in the C–H–O ternary diagram, *i.e*, steam-to-carbon ratio (S/C) < 1 at 1000 °C [12]. A large amount of steam is needed to avoid carbon deposition, while it results in the fuel dilution leading to the reduction of the fuel cell efficiency. Moreover, in the case of highly humidified hydrocarbon fuel, the degradation from the excess amount of steam during a long-term operation can be expected because thermodynamic calculations show the oxidation of Ni to NiO under high partial pressure of steam [13]. Additionally, the stability of the anode materials in redox operations (cycles of reduction and oxidation) must be addressed for the durability of performance. The high Ni volume fraction in anode material is responsible for the dimensional instability and mechanical fracture of the entire cell during redox cycles because Ni species repeatedly expand and shrink. Consequently, the anodes based on doped-$SrTiO_3$ with low nickel content have a feasibility to replace the conventional Ni-based anodes with respect to the stability under humidified methane fuel and redox conditions. Although many studies have been reported in terms of merits of the electron-conductive ceramic and its composites as anode materials, the comparative study between ceramic-based and Ni-based anodes on the stability under various severe circumstances has been scarcely carried out [14,15].

The main goal of this study is to examine the stability of YST–SDC anodes with the impregnated Ni catalyst under severe conditions comparing with the conventional Ni-based anodes. The effects of impregnated Ni catalyst in the ceramic on catalytic activity and tolerance to coking of the composites were investigated. In addition, the anodic characteristics and the corresponding cell performance were evaluated under humidified methane fuel with low S/C, highly humidified hydrogen fuel, and redox conditions.

## 2. Experimental

### 2.1. Preparation of YST–SDC composite and impregnation method

Sample powders of YST ($Y_{0.08}Sr_{0.88}TiO_3$), SDC ($Ce_{0.8}Sm_{0.2}O_{1.9}$), and YST–SDC were synthesized by following the same procedure in the previous study [11]. The YST–SDC composite powder (45 wt% SDC) was impregnated with the aqueous solution of $Ni(NO_3)_2 \cdot 6H_2O$ (Wako Pure Chemical Industries), followed by thermal decomposition at 850 °C in air to form the composite with NiO loadings of 10 and 20 wt%. The samples were prepared with 45 wt% SDC throughout this study.

The conventional Ni-based composites of Ni–YSZ and Ni–SDC were prepared from mechanical powder mixing method. The commercial powders of NiO (Wako Pure Chemical Industries) with a mean diameter of 3 μm and YSZ (Tosoh Japan) were used as starting materials. For SDC, the powder was prepared by ammonia co-precipitation technique (CP) starting with nitrate solution. The powders were initially prepared by ball-milling these powders in the ratio of 55 wt% NiO under a dry condition for 24 h. Subsequently, the well-mixed powder was calcined at 1200 °C for 5 h with the constant heating and cooling rates of 200 °C $h^{-1}$.

### 2.2. Observation of the reduction behavior

Temperature-programmed reduction (TPR, BELCAT-B, BEL Japan, Inc.) was carried out in a conventional fixed-bed flow reactor to examine the reduction behavior of the composites. The samples of YST–SDC and YST–SDC impregnated with NiO (hereafter denoted as Ni/YST–SDC) with 45 wt% SDC were heated with a supply of gaseous mixture of 4% $H_2$–Ar from room temperature to 1000 °C at a constant heating rate of 10 °C $min^{-1}$. In the reduction process, the generated steam was removed by the use of molecular-sieve trap prior to gas analysis.

### 2.3. Observation of carbon deposition behavior

The composite powders were subjected to a twice-firing at 1200 °C and 1400 °C in air for 5 h, respectively, as identical to the condition of anode preparation. The sample at a certain amount was gradually heated to 1000 °C with the heating rate of 10 °C $min^{-1}$. After the reduction with $H_2$ (10 ml $min^{-1}$), the weight change by the deposited carbon was monitored (TG, Shimadzu, TGA-50) with a supply of gaseous mixture of 30% $CH_4$–$N_2$ at 1000 °C for 1 h by thermogravimetry.

### 2.4. Electrochemical performance and stability tests

The electrochemical performance of the single cells with the composite powders as anodes was evaluated. The composite powders (with/without NiO impregnation) were mixed with polyethyleneglycol to prepare the slurry. The slurry was screen-printed on the center of YSZ disk (thickness: 500 μm, Tosoh) before firing at 1400 °C for 5 h in air. For the fabrication of cathode, the perovskite oxide of $(La_{0.8}Sr_{0.2})_{0.98}MnO_3$ (LSM) was applied in the form of slurry on the other side of YSZ before firing at 1150 °C for 5 h in air. The effective area of both electrodes was approximately 0.28 $cm^2$. Platinum wire was attached as a reference electrode to surround the side edge of YSZ disk, fixed with Pt paste, and fired at 900 °C for 2 h in air. The fabricated cell was sandwiched between alumina tubes with glass sealant. Prior to the cell testing, the anode was reduced for 30 min in a dry hydrogen atmosphere. The cell performance was evaluated with a supply of humidified hydrogen (0–40% $H_2O$) or methane with S/C of 0.1 as a fuel. The anode was exposed to the fuel gas with a flow rate of 100 ml $min^{-1}$ and oxygen was fed to the cathode as an oxidant at the same flow rate. The performance stability was evaluated mainly in severe conditions such as the exposure to methane with low S/C ratio, in highly-humidified hydrogen, and the redox cycling tests. For the evaluation of tolerance to carbon deposition, the cell was discharged at a constant current density of 0.05 A $cm^{-2}$ under humidified methane ($CH_4$–$H_2O$–$N_2$, S/C = 0.1) for 100 h. The short-term stability in highly-humidified hydrogen fuel was examined by discharging the cell at 0.1 A $cm^{-2}$ with a supply of 40% $H_2O$–$H_2$ fuel for 50 h. The conventional cells with Ni–SDC and Ni–YSZ (55 wt% NiO) anodes were evaluated for comparison. Additionally, the redox behavior of the cell was tested by alternating exposures of the anode to the reducing (5% $H_2O$–$H_2$) and oxidizing (dry air) conditions by following the previous study [16]. Before and after

oxidation treatments, the supplied gases in the anode compartment were replaced with nitrogen (100 ml $min^{-1}$) for 5 min to avoid the mixing of gaseous species. The anode was supplied with 5% $H_2O$–$H_2$ mixture for the reduction and the cell voltage was monitored under the constant current loading of 0.3 A $cm^{-2}$ for 40 min. Then, the current loading was stopped and the supplied gas was switched to dry air for 10 min to assure the complete oxidation of the anode. In this study, the redox cycles were repeated consecutively ten times. The electrochemical property was analyzed by a potentiostat/galvanostat (Solartron Analytical 1470E) and a frequency response analyzer (Solartron Analytical 1400). Impedance spectra were analyzed in a frequency range of 0.1 Hz–1 MHz with voltage amplitude of 10 mV under the open circuit condition. The microstructures of the anode before and after the operations were observed by a Scanning Electron Microscope (SEM, Carl Zeiss, NVision40) with Energy-Dispersive X-ray spectrometer (EDX).

## 3. Results and discussion

### 3.1. Microstructure of the composites

The microstructure of Ni/YST–SDC composite after reduction treatment at 1000 °C for 30 min is shown in Fig. 1. It has reported the particles with terrace and smooth surface attributed to YST and SDC, respectively, in the YST–SDC composite [11]. In this study, as the incorporated NiO into the YST–SDC composite was increased to 20 wt%, the Ni particles tended to be agglomerated to the larger size up to 2 μm as compared to Ni/YST–SDC (10 wt% NiO) composite. The elemental analysis by EDX clearly indicates the separation of each component and the good distribution of electronic and ionic conducting phases.

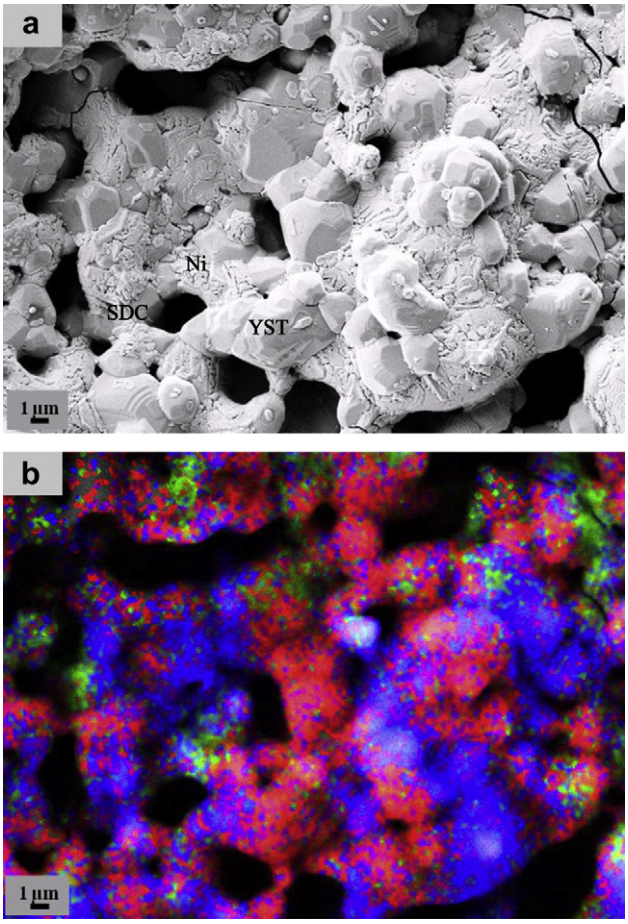


**Fig. 1.** (a) SEM image and (b) EDX mapping image of Ni/YST–SDC (20 wt% NiO) composite after reduction in humidified hydrogen (3% $H_2O$) at 1000 °C for 30 min. The green, red and blue parts correspond to Ni, Ti, and Ce, respectively.

### 3.2. Reduction behavior of the composites

Reduction behavior of YST–SDC and Ni/YST–SDC composites was investigated by TPR as shown in Fig. 2. The TPR profiles of YST, SDC, and Ni–SDC (55 wt% NiO) were observed for comparison. TPR measurement is an effective method to evaluate the chemical interaction between metal and support materials by examination of the reducibility of the catalyst such as NiO–YSZ composite [17,18]. The higher the reduction peak appears, the stronger the chemical interaction between components is. The TPR profile of SDC showed the broad peaks at 400 °C and 700 °C, which were mainly attributable to the reduction of surface and bulk of ceria in the SDC, respectively. The reduction of $Ti^{4+}$ to $Ti^{3+}$ was observed in the YST profile at 300 °C. For YST–SDC composite, the profile indicated two reduction regions corresponding to the YST and SDC at low and high temperatures, respectively. The reduction peak of SDC in the composite shifted to the higher temperature region at around 900 °C. This suggested that YST and SDC should partially interact each other. For the composites containing NiO, several reduction peaks were observed. The reduction profiles were found to be affected by the composition of NiO in the composite. It was reported that the peak at lower temperature could be assigned to the surface reduction of the NiO with less interaction with the support [18]. The result indicated that reduction of Ni/YST–SDC (10 wt% NiO) proceeded to an appreciable extent at *ca.* 600 °C and *ca.* 850 °C. The peak at higher temperature region suggested the dispersion of NiO particles with intimate contact to the YST–SDC composite. In addition, the differences in the TPR profiles depending on the NiO contents were attributed to the presence of

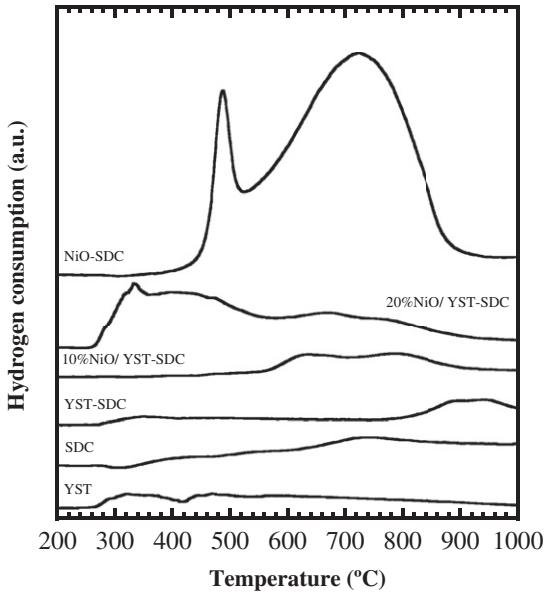


**Fig. 2.** TPR profiles of YST, SDC, YST–SDC, Ni/YST–SDC (10 wt% and 20 wt% NiO) and NiO–SDC (55 wt% NiO) with a supply of 4% $H_2$–Ar (10 $cm^3$ $min^{-1}$) mixture. The composition of SDC in the composites was kept constantly at 45 wt% and the samples were calcined at 1400 °C for 5 h prior to their measurement.

distinct states of the NiO in the composites. The reduction of surface and bulk of NiO and SDC at *ca.* 500 °C and *ca.* 700 °C, respectively, was clearly observed from the reduction profile of NiO–SDC.

### 3.3. Carbon deposition behavior

Carbon deposition behavior over the as-calcined composites was evaluated by TG analysis. After the reduction with $H_2$ (10 ml $min^{-1}$), the weight increase by the deposition of carbon was monitored at 1000 °C for 1 h during a supply of $CH_4$–$N_2$ gaseous mixture in a dry condition. Fig. 3 shows the time course of weight change over the composites of YST–SDC, Ni/YST–SDC (10 wt% and 20 wt% NiO). The weight change over the cermet of Ni–SDC was also illustrated for comparison. In a dry condition, the formation of carbon can be suggested from methane pyrolysis (Equation (1)).

$$CH_4 \rightarrow C + 2H_2 \quad (1)$$

The results showed that the amount of deposited carbon over the samples gradually increased with the distinctive rate. The amount of deposited carbon was found to be dependent on the amount of Ni catalysts in the composite. The higher amount of deposited carbon can be expected for the composite with the abundant surface area of Ni metal in the composite. Accordingly, carbon deposition was significantly promoted over the Ni–SDC (55 wt% NiO) cermet. On the contrary, the composites of YST–SDC and Ni/YST–SDC (10 wt% and 20 wt% NiO) showed the relatively low deposition due to the advantages of YST as an inactive ceramic-based material for carbon deposition [19]. The composites of Ni/YST–SDC (10 wt% and 20 wt% NiO) exhibited the comparable rate of carbon deposition during the first 30 min. This was because the agglomeration of nickel particles in the composite with higher Ni content greatly reduced the surface area of metallic nickel.

### 3.4. Electrochemical performance

To evaluate the electrochemical performance, the composite powders of YST–SDC and Ni/YST–SDC were applied as anode materials in the single cells. The LSM cathode was used for the tested cells. Fig. 4 shows *I–V* and *I–P* characteristics of the single cells with various compositions of Ni/YST–SDC anodes operated in methane fuel with S/C = 0.1 at 1000 °C. The amount of SDC in the composites was kept at 45 wt% throughout the study. The performance of Ni–SDC was also illustrated for comparison. According to the experimental results, the amount of Ni catalyst was an important factor for the electrochemical performance with the use of methane fuel. In general, nickel is a well-known catalyst for the reforming of methane. The increased OCVs as compared with those measured in hydrogen fuel were found in the Ni-contained anodes, which clearly indicated the formation of carbon from the decomposition reactions of the methane fuel at high temperatures [20]. The composite of Ni/YST–SDC (20 wt% NiO) could attain high performance of *ca.* 280 mW/$cm^2$, while the anode without Ni showed relatively low performance of *ca.* 55 mW/$cm^2$. However, the performance achieved is still lower than that of the Ni–SDC anode. This result concluded that the performance enhancement should be accomplished by an increase in Ni content.

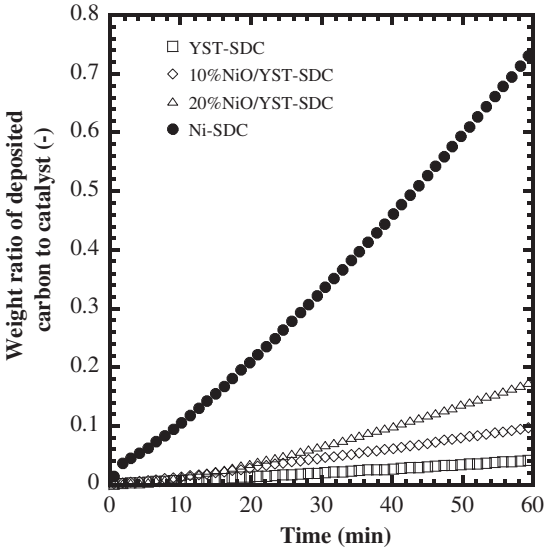


**Fig. 3.** Time course of weight change for the composites of YST–SDC, Ni/YST–SDC (10 wt% and 20 wt% NiO), and Ni–SDC (55 wt% NiO) with a supply of dry methane at 1000 °C for 1 h.

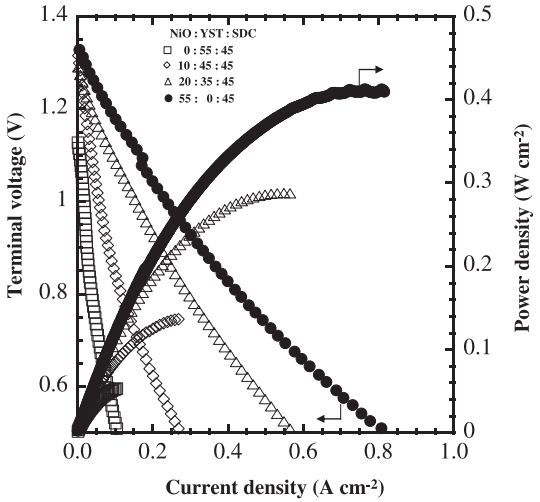


**Fig. 4.** *I–V* and *I–P* characteristics of the single cells with YST–SDC (55 wt% YST, *square*), Ni/YST–SDC (10 wt% NiO, *diamond*), Ni/YST–SDC (20 wt% NiO, *triangle*), and Ni–SDC (55 wt% NiO, *circle*) anodes operated at 1000 °C in humidified methane fuel (S/C = 0.1). Cathode: LSM, electrolyte: YSZ. The composition of SDC in the composites was kept at 45 wt%.

### 3.5. Stability in methane fuel

To replace the conventional Ni-based anodes with YST–SDC-based anodes, the amount of Ni additive into anode material should be restricted. From the experimental results mentioned above, the composite of Ni/YST–SDC with 20 wt% NiO was selected as a promising candidate for the further study. The performance stability of the cell with this composite anode was evaluated during the discharge at 0.05 A $cm^{-2}$ with methane fuel (S/C = 0.1) at 1000 °C by comparison with Ni–SDC anode. Fig. 5 shows the time course of terminal voltage for the cells with Ni/YST–SDC and Ni–SDC anodes. The cell with Ni–SDC anode initially exhibited the superior performance to the Ni/YST–SDC anode. However, performance was gradually degraded by about 7% over the operating period. According to the previous results observed by TG, Ni–SDC showed comparatively high deposition rate of carbon within 1 h. From this reason, the degradation factor was ascribable to the carbon deposited mainly over the nickel catalyst in the Ni–SDC composite. Ni/YST–SDC anode attained more stable performance in this severe condition, although the electrocatalytic activity of this composite was not high as compared with the conventional Ni-

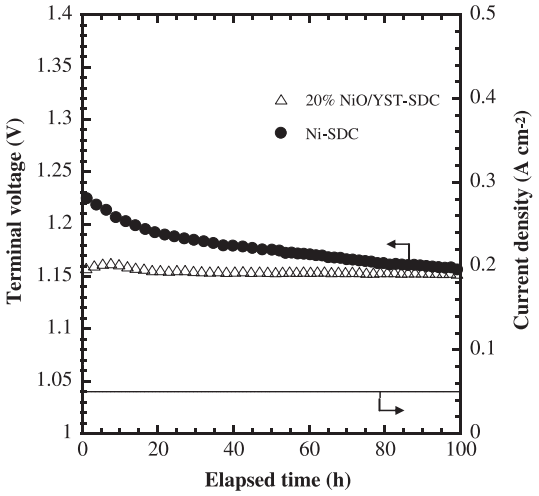


**Fig. 5.** Time course of terminal voltage for the single cells with Ni/YST–SDC (20 wt% NiO, *triangle*) and Ni–SDC (55 wt% NiO, *circle*) anodes during a discharge at a constant current of 0.05 A $cm^{-2}$ in methane fuel (S/C = 0.1) operated at 1000 °C for 100 h. Cathode: LSM, electrolyte: YSZ.

based material. Despite the use of low-humidified methane fuel (S/C = 0.1), the coke formation over Ni catalyst had an insignificant impact on the cell performance. The performance was gradually increased and kept stable over the discharged period. For Ni/YST–SDC (10 wt% NiO) anode, the previous studies have reported the stable performance over 20 h in the same condition [11]. In this study, the stable performance could be also achieved even with higher amount of NiO over the prolonged operating time up to 100 h. Thus, this composite offers remarkably high tolerance to carbon deposition, considering the high Ni content up to 20 wt%. In addition, the performance of Ni/YST–SDC anode was comparable to that for Ni–SDC (55 wt% NiO) anode after 100 h from the start of operation.

### 3.6. Stability in highly humidified hydrogen fuel

To evaluate the contribution of steam to the electrochemical performance of Ni/YST–SDC (20 wt% NiO) anode, the single cell was tested under hydrogen fuel with various steam contents to the anode. Fig. 6 shows *I–V* and *I–P* characteristics of the cell in hydrogen fuel with 0–30% of steam at 1000 °C. The OCV values measured in all conditions were approximately close to the theoretical ones indicating that gas leak was not found. Due to the deficiency of steam, the significant voltage drop was observed at the low current density under the dry condition. The cell performance was reduced with the rise of steam contents in hydrogen fuel because of the difference in chemical potential observed in the OCV for each fuel.

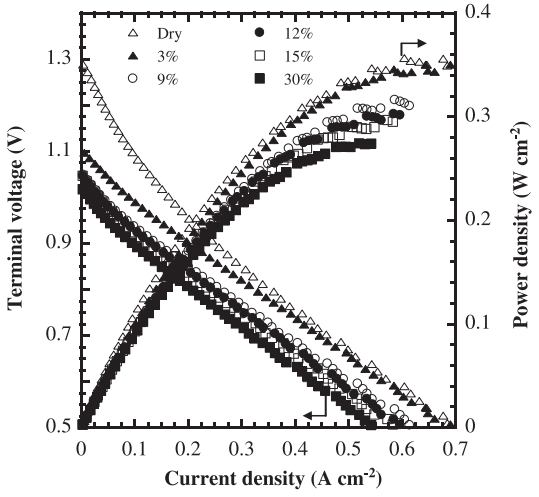


**Fig. 6.** *I–V* and *I–P* characteristics of the single cell with Ni/YST–SDC anode (20 wt% NiO) operated at 1000 °C in hydrogen fuel with various percentages of steam. Cathode: LSM, electrolyte: YSZ.

The effect of steam content on the hydrogen oxidation over YST–SDC and Ni/YST–SDC anodes was examined. In the impedance spectra measured at OCVs, the intercept of the impedance arcs with the real axis at high frequencies corresponds to the ohmic resistance ($R_o$), and the overall size of the arcs is assigned to the anode polarization resistance ($R_p$). The changes in $R_p$ and $R_o$ depending on the humidity in hydrogen fuel are illustrated in Fig. 7. The ohmic resistance of the cell indicated the humidity independence for all composite anodes, while the anode polarization resistance was greatly affected by the change of $p(H_2O)$. The obvious resistance drop by the introduction of Ni catalyst was observed. In each condition, the higher polarization resistance appeared with the use of dry hydrogen fuel. However, the polarization resistances were reduced significantly as 3% of steam was introduced into the hydrogen fuel. The oxidation of hydrogen was strongly influenced by the electrocatalytic activities of the composite anodes in the presence of water as the moist gas affected the surface reactions. Jiang et al. [21] reported the indispensability of steam (up to 2%) in the hydrogen fuel stream which substantially promoted the adsorption of hydrogen on the active sites of Ni-based anode. However, the increase in $R_p$ was observed at the highly humidified hydrogen fuel as shown in Fig. 7. In general, the polarization resistance depends strongly on the number of electrocatalytic active sites and the concentration of gases near the triple phase boundary. Thus, this increase in the resistance should be attributed to the change of gas concentration.

Furthermore, the short-term stability of the single cells with Ni/YST–SDC (20 wt% NiO) and conventional Ni–YSZ anodes was evaluated during discharge at 0.1 A $cm^{-2}$ in hydrogen fuel with 40% of steam at 1000 °C for 50 h. Fig. 8 shows the time courses of terminal voltage for the single cells with respective anodes. The results clearly indicated that the cell with Ni–YSZ anode showed

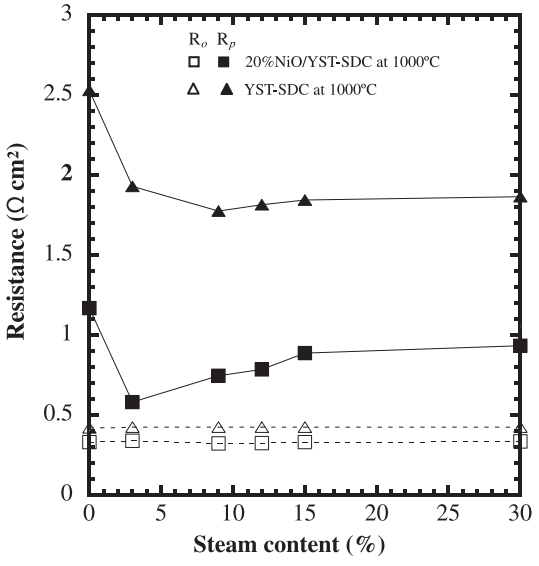


**Fig. 7.** Anode polarization ($R_p$) and ohmic ($R_o$) resistances of YST–SDC and Ni/YST–SDC (20 wt% NiO) in hydrogen fuel with various percentages of steam at 1000 °C.

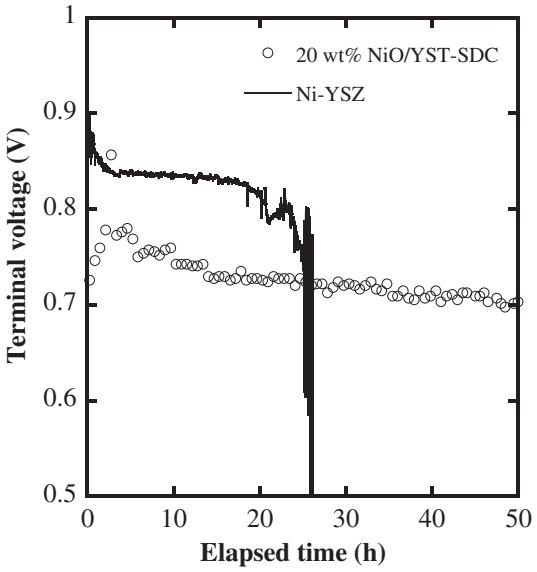


**Fig. 8.** Time course of terminal voltage of the single cells with Ni/YST–SDC (20 wt% NiO) and Ni–YSZ (55 wt% NiO) anodes during a discharge at 0.1 A $cm^{-2}$ in humidified hydrogen (40% $H_2O$–60% $H_2$) operated at 1000 °C. Cathode: LSM, electrolyte: YSZ.

relatively high performance compared with the Ni/YST–SDC anode due to the higher content of nickel component. However, the performance gradually decreased during the discharged period and then suddenly deteriorated in 25 h which was in accordance with the previous study of Matsui et al. [22]. According to the previous results, the degradation of the performance strongly depended on the humidity of fuel as the steam deactivated the surface of Ni. In this study, the cell was discharged for longer period due to the lower current density by comparison with the previous study. For Ni/YST–SDC anode, the increase of cell voltage at the initial stage is attributable to the effect of current passing on cathode electrode and the performance appears to degrade gradually over the discharge period due to the negative effect on nickel surface. Regardless of the same operating conditions, the cell with

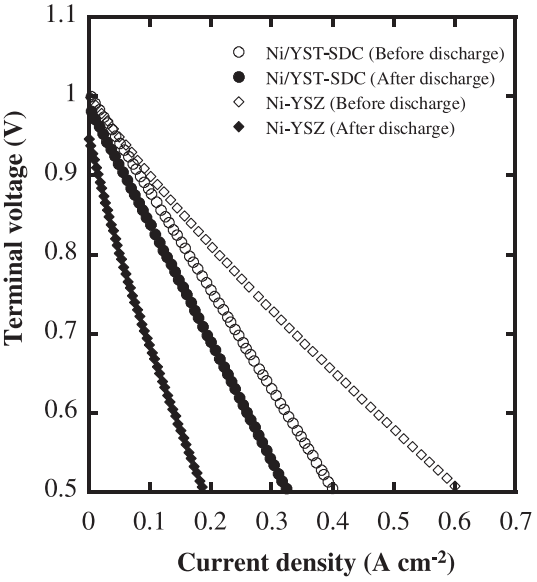


**Fig. 9.** *I–V* characteristics of the single cells with Ni/YST–SDC anode (20 wt% NiO) and Ni–YSZ (55 wt% NiO) anodes before and after discharge at 0.1 A $cm^{-2}$ in humidified hydrogen (40% $H_2O$) operated at 1000 °C. Cathode: LSM, electrolyte: YSZ.

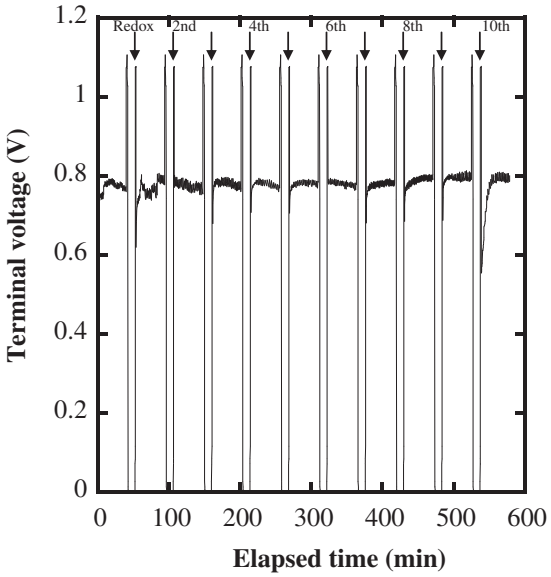


**Fig. 10.** Time course of terminal voltage of the single cell with Ni/YST–SDC (20wt% NiO) anode during the redox cycles at 1000 °C. The cell was discharged at 0.3 A $cm^{-2}$ in humidified $H_2$ (5% $H_2O$–95% $H_2$) for 40 min before the supply of dry air for 10 min in each cycle.

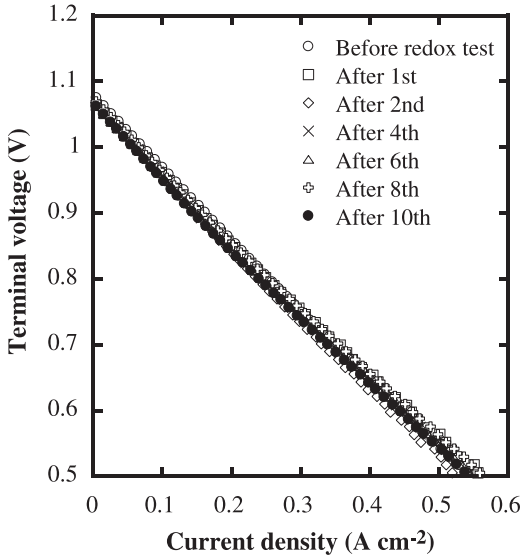


**Fig. 11.** *I–V* characteristics of the single cells with Ni/YST–SDC anode (20 wt% NiO) before redox treatment and after the 1st, 2nd, 4th, 6th, 8th, and 10th redox cycles with the alternating supply of humidified $H_2$ (5% $H_2O$–95% $H_2$) for 40 min and dry air for 10 min in each cycle.

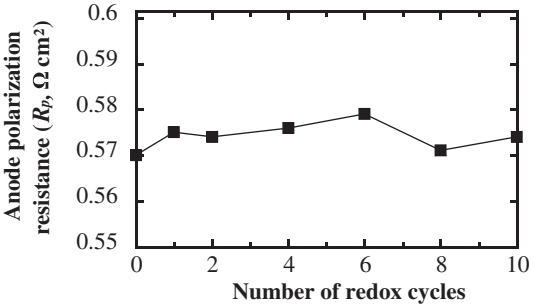


**Fig. 12.** Anode polarization resistance ($R_p$) of Ni/YST–SDC anode (20 wt% NiO) before redox treatment and after the 1st, 2nd, 4th, 6th, 8th, and 10th redox cycles.

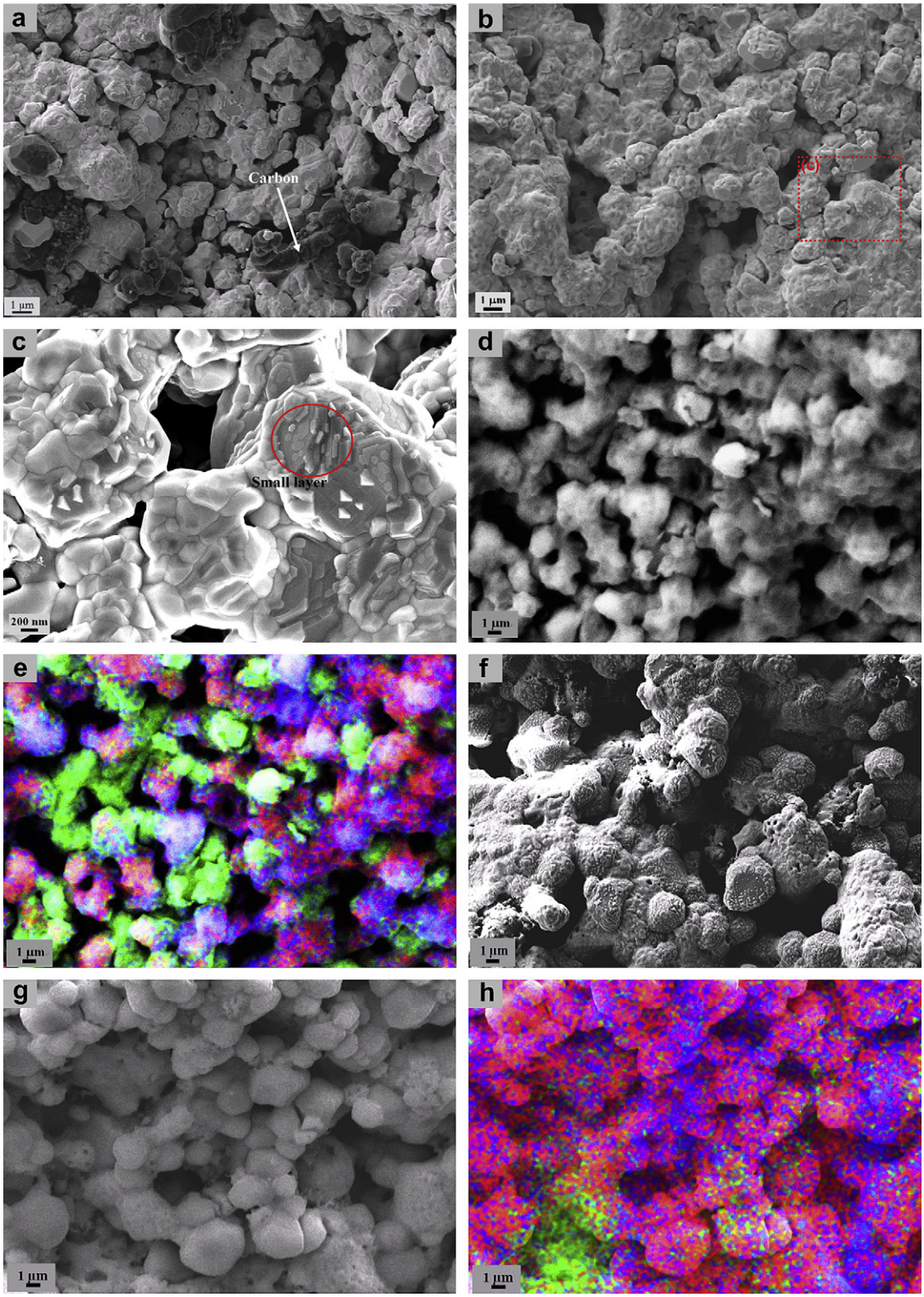


**Fig. 13.** SEM images of the Ni/YST–SDC anode (20 wt% NiO) after the stability tests: (a) discharge at 0.05 A $cm^{-2}$ in humidified methane fuel (S/C = 0.1) for 100 h; (b–e) discharge at 0.1 A $cm^{-2}$ in highly humidified $H_2$ (40% $H_2O$) for 50 h; (d) SEM and (e) EDX mapping images; (f–h) 10th redox cycling test between dry air and hydrogen; (g) SEM and (h) EDX mapping images. The green, red and blue parts correspond to Ni, Ti, and Ce, respectively.

Ni/YST–SDC anode could attain the higher tolerance over the operating period because of the lower negative effect on the nickel surface. Fig. 9 shows the *I–V* characteristics of the cells with both anodes before ($t = 0$ h) and after the discharge period ($t = 50$ h or after performance deterioration). After the discharge in highly humidified hydrogen, the performance decreased by about 68% and

20% from the maximum power density at 0.5 V achieved during the initial operation of the cells with the Ni–YSZ and Ni/YST–SDC anodes, respectively.

### 3.7. Stability upon redox cycle

Since the high volume fraction of Ni in the anode material causes a mechanical fracture of the cell by alternating exposure to oxidizing and reducing atmospheres [23,24], the conventional Ni-based anode-supported cell showed obvious losses of OCV and performance due to the failure from a large volume change after just one redox cycle. Thus, the redox stability of the alternative ceramic anode should be investigated. Redox cycling test of the cell with Ni/YST–SDC anode was conducted at 1000 °C. Fig. 10 shows the change of terminal voltage during the redox cycles by alternating supply of dry air and hydrogen to the anode. *I–V* characteristics and anode polarization resistance before and after each redox cycling test were measured as shown in Figs. 11 and 12, respectively. The result indicated that the cell voltage became zero immediately after the supply of dry air to oxidize the anode. However, the open-circuit voltage (OCV) was recovered to 1.07 V after switching to hydrogen fuel in each cycle, which agreed well with the theoretical value calculated from the Nernst equation. After the redox cycle, the cell voltage degraded during discharge could almost recover to that of the initial condition. In the previous study on the Ni–YSZ anode, the obvious degradation was confirmed by impedance measurement after the 4th redox cycling [16]. The significant increase in polarization resistance of Ni–YSZ anode by *ca.* 67% from the initial value was observed, while that of Ni/YST–SDC anode slightly rose by *ca.* 0.89% after the 4th redox cycle. The increase in polarization resistance of the anode suggests that the loss of the reaction sites for the electrochemical oxidation of hydrogen fuel upon the redox treatment. Accordingly, the Ni/YST–SDC anode had the advantage of superior stability in redox conditions to the conventional Ni–YSZ anode. Recently, Ikebe et al. have reported the high durability of performance for 10 wt% Ni/YST–YSZ anode in five consecutive redox cycles due to the advantage of YST–YSZ ceramic framework [6]. In this study, the restoration of performance after subsequent reduction treatment was confirmed by the insignificant change of *I–V* characteristics and the polarization resistance of Ni/YST–SDC anode after the consecutive redox up to 10 cycles. Consequently, with YST–SDC ceramic framework, the dimensional change of Ni particles associated with the redox cycling had no detrimental damage on the cell performance.

### 3.8. Microstructure after the stability tests

Fig. 13 shows FE–SEM and energy-dispersive X-ray (EDX) mapping images of Ni/YST–SDC (20 wt% NiO) after the stability tests in humidified methane and hydrogen, and redox cycle. As Ni catalyst promotes the formation of carbon, Fig. 13 (a) shows the existence of carbon extensively over the Ni/YST–SDC composite after the operation with methane fuel. However, these carbonaceous species insignificantly affected the cell performance over the prolonged operation up to 100 h as shown in Fig. 5. This was ascribed to the higher carbon tolerance of the Ni/YST–SDC composite. For the operation with highly humidified hydrogen fuel, some laminated deposits over the particles led to the rough surface as shown in Fig. 13 (b) and (c), which may possibly affect the performance degradation during the discharge period. The drastic change should be observed mainly on the Ni particles because the adsorption of steam proceeds preferentially on the Ni surface to oxidize Ni species [21]. In Fig. 13 (d) obtained with elemental analysis, the red, blue, and green regions correspond to the components of Ti (YST), Ce (SDC), and Ni, respectively. The Ni particles agglomerated extensively in the composite after the stability test as illustrated in Fig. 1 (b). Consequently, a small degradation could be observed in the Ni/YST–SDC anode operated in high percentage of steam as shown in Fig. 8. Similar surface morphology could be observed in the Ni/YST–SDC (20 wt% NiO) composite after the consecutive redox cycle as shown in Fig. 13 (f)–(h). The surface morphological change was found in the composite after the redox cycling test as shown in Fig. 13 (f). It is well-known that the dimensional change upon the reduction and oxidation of Ni in the anode leads to the severe fracture either of the anode itself or of the electrode–electrolyte interface. In this study, due to the advantages of YST–SDC ceramic framework with low nickel contents, no cracks or fracture were observed in the composite. Recently, Sumi et al. have reported the agglomeration of the deformed Ni particles during the redox cycles of Ni–YSZ anode would be ascribed to a key reason for the performance degradation [16]. However, the microstructure of Ni/YST–SDC (20 wt% NiO) indicates that the dimensional change and/or coarsening of Ni phase did not proceed remarkably due to the good framework of the ceramic material resulting in the insignificant change in performance under the redox cycles.

## 4. Conclusions

The composite anodes consisting of yttria-doped $SrTiO_3$ (YST) and SDC incorporated with NiO were prepared to evaluate the stability of electrocatalytic performance comparing with the conventional Ni-based anodes. The addition of NiO up to 20 wt% into YST–SDC composite enhanced the electrocatalytic activity. The cell with Ni/YST–SDC anode attained the excellent and stable performance even in the operation with humidified methane at S/C = 0.1 for 100 h without the deterioration from carbon deposition. The stable performance suggested the Ni/YST–SDC anode with low nickel content suppressed carbon deposition effectively. Moreover, Ni/YST–SDC anode showed the higher tolerance in the operation with highly humidified fuels and redox cycle. According to these results, the composite of Ni/YST–SDC comparatively accomplished a good performance and stability as an alternative anode material operated in various severe circumstances.

## References

[1] L. Yang, S.Z. Wang, K. Blinn, M.F. Liu, Z. Liu, Z. Cheng, M.L. Liu, Science 326 (2009) 126.
[2] J.B. Wang, H.C. Jang, T.J. Huang, J. Power Sources 122 (2003) 122.
[3] O.A. Marina, N.L. Canfield, J.W. Stevenson, Solid State Ionics 149 (2002) 21–28.
[4] J.T. Vaughey, J.R. Mawdsley, T.R. Krause, Mater. Res. Bull. 42 (2007) 1963.
[5] J.C. Ruiz-Morales, J. Canales-Vazquez, D. Marrero-lopeZ, J.T.S. Irvine, P. Nunez, Electrochim. Acta 52 (2007) 7217.
[6] T. Ikebe, H. Muroyama, T. Matsui, K. Eguchi, J. Electrochem. Soc. 157 (2010) 970.
[7] S. Hui, A. Petric, Mater. Res. Bull. 37 (2002) 1215.
[8] X. Huang, H. Zhao, W. Shen, W. Qin, W. Wu, J. Phys. Chem. Solids 67 (2006) 2609.
[9] X. Li, H. Zhao, F. Gao, Z. Zhu, N. Chen, W. Shen, Solid State Ionics 179 (2008) 1588.
[10] X.F. Sun, R.S. Guo, J. Li, Ceram. Int. 34 (2008) 219.
[11] P. Puengjinda, H. Muroyama, T. Matsui, K. Eguchi, J. Power Sources 204 (2012) 67.
[12] K. Sasaki, Y. Teraoka, J. Electrochem. Soc. 150 (2003) 885.
[13] S. Koch, P.V. Hendriksen, M. Mogensen, Y.L. Liu, N. Dekker, B. Rietveld, B. de Haart, F. Tietz, Fuel Cells 06 (2006) 130.
[14] J.W. Miao, Y.N. Fan, Y.Sh. Jin, Chem. Ind. Times 17 (2003) 21.
[15] S. Hui, A. Petric, J. Electrochem. Soc. 149 (2002) J1.
[16] H. Sumi, R. Kishida, J.Y. Kim, H. Muroyama, T. Matsui, K. Eguchi, J. Electrochem. Soc. 157 (2010) B1747.
[17] W.S. Dong, H.S. Roh, K.W. Jun, S.E. Park, Y.S. Oh, Appl. Catal. A 226 (2002) 63.
[18] H. Mori, C.J. Wen, J. Otomo, K. Eguchi, H. Takahashi, Appl. Catal. A 245 (2003) 79.
[19] M.R. Pillai, I. Kim, D.M. Bierschenk, S.A. Barnett, J. Power Sources 185 (2008) 1086.
[20] K. Kendall, C.M. Finnerty, G. Saunders, J.T. Chung, J. Power Sources 106 (2002) 323.
[21] S.P. Jiang, S.P.S. Badwal, J. Electrochem. Soc. 144 (1997) 3777.
[22] T. Matsui, R. Kishida, J.Y. Kim, H. Muroyama, K. Eguchi, J. Electrochem Soc. 157 (5) (2010) B776.
[23] G. Stathis, D. Simwonis, F. Tietz, A. Moropoulou, A. Naoumides, J. Mater. Res. 17 (2002) 951.
[24] J. Malzbender, E. Wessel, R.W. Steinbrech, Solid State Ionics 176 (2005) 2201.